Proceedings of the 2007 American Control Conference
Marriott Marquis Hotel at Times Square
New York City, USA, July 11-13, 2007

ThA01.4

Vision-Based Leader/Follower Tracking for Nonholonomic Mobile Robots

Hariprasad Kannan, Vilas K. Chitrakaran, Darren M. Dawson and Timothy Burg

Abstract— **This paper presents a strategy for a nonholonomic mobile robot to autonomously follow a target based on vision information from an onboard pan camera unit (PCU). Homography-based techniques are used to obtain relative position and orientation information from the monocular camera images. The proposed kinematic controller, based on the Lyapunov method, achieves uniform ultimately bounded (UUB) tracking.**

I. INTRODUCTION

Autonomous guided vehicles (AGVs) have found a variety of commercial applications. In industry, AGVs are utilized primarily for material handling. Typically, such vehicles have utilized laser/sonar rangefinders, optical sensors, or magnetic guidance systems for navigation through constrained environments. More recently, owing to the increase in computing power of commercial off-the-shelf computers, it has become possible to process data from information rich sensors such as a standard video camera, for guidance and navigation of vehicles. For example, vision-based systems for autonomous motion control of ground vehicles in urban environments have been developed (e.g., The California PATH program [9]). Research in this area also has implications for technological progress in assistive and rehabilitation robotics as well [15]. In addition, many applications require autonomous ground vehicles to move in a formation, for example, exploring remote locations, surveillance, and enclosing a target [14]. To this end, various approaches to formation control and utilizing vision in navigation have emerged. For instance, [4] investigates a graph theory based approach to formation control. A vision-based solution to formation control is presented in [3]. In [12], an Extended Kalman Filter is applied to visual data to achieve leader/follower tracking. A nonlinear tracking controller utilizing a novel sensor, namely an omnidirectional camera, is presented in [18]. The work in [13] demonstrates a Lyapunov-based output feedback approach to formation control.

In this paper, we present a Lyapunov-based approach to vision-based leader/follower tracking for nonholonomic mobile robots equipped with a monocular calibrated camera mounted on a controllable pan unit. Such an approach views the formation control problem as a combination of several similar local control problems requiring each follower to track its assigned leader. The tracking objective requires information related to the leader's motion, which is extracted from the video stream captured by the follower camera. This type of camera-based solution eliminates the need for any sophisticated communication between the leader and the follower; furthermore, models for the leader's motion and/or the leader's geometric configuration are not required. Specifically, a reference image is initially captured when the follower is at the desired position and orientation relative to the leader. If the current image captured by the follower coincides with the reference image as the leader is in motion, the control objective is achieved. To perform this visual servoing task, we utilize the homography-based approach (also called $2\frac{1}{2}$D visual servoing [11]) to quantify motion in Euclidean space by utilizing image space information (i.e., image coordinates of features on the leader). Along this line of reasoning, the development in [1] describes an algorithm to track prerecorded images of a fixed target generated by a nonholonomic mobile robot. In contrast to [1], the proposed controller is different because the target image (i.e., the leader) is moving; furthermore, it must be emphasized that the motion of the leader need not be nonholonomic. Therefore, tracking can be achieved for a wider range of leader motions. As one might expect, unconstrained motion on a plane requires a vehicle with three degrees of freedom (d.o.f), two for position and one for orientation. The follower vehicle that we consider in this paper is an underactuated mobile robot; the robot is equipped with two actuators, one that enables forward motion and another that enables turning. Augmenting the robot with a pan camera unit provides an additional d.o.f that makes the robot-camera system fully actuated with respect to the task of the follower tracking the desired (reference) image of the leader. This allows us to design an integrated controller that maintains the follower robot-camera system at the desired location behind the leader. In [17], a similar approach was explored to augment the d.o.f. of a mobile robot; however, the visual servoing task utilized a different approach. A pan camera on the robot also has the additional advantage of maintaining line of sight with feature points on the leader more effectively compared to a body fixed camera (i.e., it is more likely that the target will remain in the field of view).

II. PROBLEM FORMULATION

Let us denote the inertial frame and the frame fixed on the mobile robot as I and F, respectively. The x-axis of F is along the forward direction of the robot. The robot moves on a plane parallel to the XY plane of F. It is assumed that the

origin of the camera frame, denoted by C, coincides with that of the robot frame F. The camera's optical axis is along the x-axis of C. The frames C and F are aligned when the pan angle, denoted by $\theta_p(t) \in \mathbb{R}^1$, is zero and the camera's optical axis is along the approach direction of the robot. The
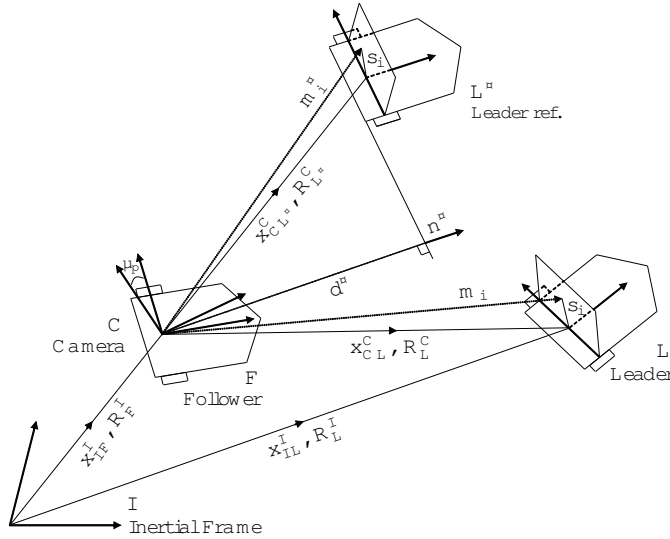

Fig. 1. Relationship between coordinate frames.

frame fixed on the leader is denoted by L. The leader moves on the same plane as the follower. Let L^* denote the fixed reference position and orientation of the leader with respect to C, captured initially by the follower camera. The z-axis of all the frames are parallel to each other and orthogonal to the plane. Figure 1 shows the spatial relationships between the various frames. The goal of this paper is to design a controller that will move the follower and the PCU such that L coincides with L^* as seen from the camera frame C.

In this paper, we will use the following convention [6]: vectors are specified as v_{eb}^n, which signifies the vector v of the b frame relative to the e frame and expressed in the n frame. $'x'$, $'v'$ and $'\omega'$ denote position, translational velocity and angular velocity, respectively. A rotation matrix is specified as $R_f^t \in SO(3)$, which transforms coordinates defined in the f frame to the t frame.

A. Geometric Model

The mobile robot's linear and angular velocities, denoted by $v_{IF}^F(t)$, $\omega_{IF}^F(t) \in \mathbb{R}^3$ respectively, can be defined as follows

$$
\begin{aligned}
v_{IF}^F &= \begin{bmatrix} v_F & 0 & 0 \end{bmatrix}^T \\
\omega_{IF}^F &= \begin{bmatrix} 0 & 0 & \omega_F \end{bmatrix}^T
\end{aligned}
\tag{1}
$$

where $v_F(t)$, $\omega_F(t) \in \mathbb{R}^1$. The angular velocity of the leader with respect to I and the angular velocity of the PCU with respect to F, denoted by $\omega_{IL}^L(t)$, $\omega_{FC}^F(t) \in \mathbb{R}^3$ respectively, are expressed as follows

$$
\begin{aligned}
\omega_{IL}^L &= \begin{bmatrix} 0 & 0 & \omega_L \end{bmatrix}^T \\
\omega_{FC}^F &= \begin{bmatrix} 0 & 0 & \omega_C \end{bmatrix}^T \\
\omega_C &= \dot{\theta}_p
\end{aligned}
\tag{2}
$$

where $\omega_L(t)$, $\omega_C(t) \in \mathbb{R}^1$.

Given the arrangement of the camera frame C and mobile robot frame F, the transformation between C and F has the following form [16]

$$
R_C^F = \begin{bmatrix} \cos\theta_p & -\sin\theta_p & 0 \\ \sin\theta_p & \cos\theta_p & 0 \\ 0 & 0 & 1 \end{bmatrix}.
\tag{3}
$$

As shown in Figure 1, the ith feature on the leader is at a constant position $s_i \in \mathbb{R}^3$ relative to L. Let $m_i(t) \triangleq \begin{bmatrix} x_i(t) & y_i(t) & z_i(t) \end{bmatrix}^T \in \mathbb{R}^3$ denote the coordinates of the same feature expressed in the follower's camera frame C. Let $x_{CL}^C \in \mathbb{R}^3$ and $R_L^C \in SO(3)$ denote the position and orientation of the leader relative to the follower camera frame C, respectively and let $x_{CL^*}^C \in \mathbb{R}^3$ and $R_{L^*}^C \in SO(3)$ denote the desired position and orientation of the leader relative to frame C, respectively. At the desired configuration, let $m_i^* \in \mathbb{R}^3$ denote the coordinates of the ith feature relative to frame C.

From Figure 1, it can be seen that $m_i(t)$ and m_i^* are defined as follows

$$
\begin{aligned}
m_i &= x_{CL}^C + R_L^C s_i \\
m_i^* &= x_{CL^*}^C + R_{L^*}^C s_i.
\end{aligned}
\tag{4}
$$
$$\tag{5}$$

Eliminating s_i from (4) and (5), we obtain

$$
m_i = \bar{x} + \bar{R} m_i^*
\tag{6}
$$

where $\bar{R}(t) \in SO(3)$ and $\bar{x}(t) \in \mathbb{R}^3$ are rotation- and translation-like variables, respectively, defined as follows

$$
\begin{aligned}
\bar{R} &= R_L^C R_C^{L^*} \\
\bar{x} &= x_{CL}^C - \bar{R} x_{CL^*}^C.
\end{aligned}
\tag{7}
$$
$$\tag{8}$$

We assume that at least four feature points tracked on the leader are selected such that they are coplanar. Let $n^* \in \mathbb{R}^3$ denote the constant unit normal from the origin of the camera frame to the feature-plane, when the leader is at L^*. Let $d^* \neq 0 \in \mathbb{R}^1$ denote the constant distance to this plane from the camera. Then d^* is the projection along n^* of all the features m_i^*, which can be expressed as follows

$$
d^* = n^{*T} m_i^*.
\tag{9}
$$

Using (9), (6) can be re-written as

$$
m_i = \underbrace{\left(\bar{R} + \frac{\bar{x}}{d^*} n^{*T} \right)}_{H} m_i^*
\tag{10}
$$

where $H(t) \in \mathbb{R}^{3\times 3}$ is an Euclidean Homography [8].

Remark 1: The four coplanar feature points required in order to compute the homography $H(t)$ may be artifially fixed on the leader vehicle. If coplanar feature points are not available and cannot be artifically fixed on the leader, $H(t)$ can still be constructed using the virtual parallax algorithm [11]. However, in this case, at least eight non-coplanar features are required.

B. Euclidean Reconstruction

We need to extract Euclidean related position and orientation information from the images of the features on the leader. The coordinates of the feature points in the camera images are represented as 2D homogeneous coordinates, denoted by $p_i(t), p_i^* \in \mathbb{R}^3$, relative to frame C. The pin-hole camera model [8] relates these to the normalized Euclidean coordinates $\frac{m_i(t)}{x_i(t)}$ and $\frac{m_i^*}{x_i^*}$ as follows

$$p_i = A \frac{m_i}{x_i} \quad p_i^* = A \frac{m_i^*}{x_i^*} \tag{11}$$

where $A \in \mathbb{R}^{3\times3}$ is a known, constant and invertible intrinsic camera calibration matrix and $x_i(t), x_i^* \in \mathbb{R}^1$ are the x-coordinates of $m_i(t)$ and m_i^*, respectively. Hence, image coordinates can be introduced into (10) as follows

$$p_i = \underbrace{\frac{x_i^*}{x_i}}_{\alpha_i} \underbrace{A H A^{-1}}_{G} p_i^* \tag{12}$$

where the depth ratio $\frac{x_i^*}{x_i(t)}$ is denoted by $\alpha_i(t) \in \mathbb{R}^1$ and $G(t) \in \mathbb{R}^{3\times3}$ is a full-ranked homogeneous collineation matrix [8]. Given a set of corresponding points $(p_i(t), p_i^*)$, the elements of $G(t)$ can be determined up to a scale factor. Since, there are eight unknowns, a minimum of four corresponding pairs are required to compute $G(t)$. Since, the intrinsic camera calibration matrix A is assumed to be known, $H(t)$ can then be uniquely determined from $G(t)$. Homography decomposition algorithms, described in [5], [8], can be used to calculate $\bar{R}(t)$ and $\frac{1}{d^*}\bar{x}(t)$ from $H(t)$. Note that it is possible to obtain only $\frac{1}{d^*}\bar{x}(t)$ and not $\bar{x}(t)$.

Remark 2: By tracking more than the required minimum of four feature points, the accuracy of estimation of the homography matrix can be improved in the presence of image noise, resulting in improved estimates for signals obtained from the subsequent decomposition of the homography.

III. CONTROL DEVELOPMENT

The control objective is to ensure that the image of the leader as seen by follower camera matches the reference image captured when the leader was at a desired position and orientation. Referring to Figure 1 and the previous section, this objective can be framed as

$$x_{CL}^C \to x_{CL^*}^C \ , \ R_L^C \to R_{L^*}^C \quad \text{as } t \to \infty. \tag{13}$$

Examining equations (7) and (8), it is seen that the above control objective is achieved, if $\bar{R}(t) \to I_{3\times3}$ and $\bar{x}(t) \to 0$ as $t \to \infty$, where $I_{n\times n}$ denotes an $n \times n$ identity matrix.

We develop the control inputs $v_F(t), \omega_F(t), \omega_C(t)$ based on the measurable signals $\bar{R}(t)$, $\frac{1}{d^*}\bar{x}(t)$ and $\theta_p(t)$. To facilitate the control development, we make the following assumptions

Assumption 1: The pan angle of the PCU (i.e., $\theta_p(t)$) is measurable using suitable sensors like encoders. Hence, we can compute $R_C^F(t)$ using (3), which is required in the control development.

Assumption 2: The kinematic variables of the leader are bounded i.e., $x_{IL}^I(t), v_{IL}^I(t), \omega_{IL}^I(t) \in \mathcal{L}_\infty$. Since, there is

no communication between the robots, these signals are not available to the controller on the follower robot.

Assumption 3: The mechanical dynamics of the follower robot and the PCU can be neglected.

Assumption 4: The follower robot is always behind the leader and the features on the leader are always within the field of view of the follower's camera.

A. Open-loop Error System

The orientation error, denoted by $e_\theta(t) \in \mathbb{R}^3$, is defined in terms of the axis-angle representation of the rotation matrix $\bar{R}(t)$, given in (7), as follows [16]

$$e_\theta \triangleq \mu\phi \tag{14}$$

where $\mu(t) \in \mathbb{R}^3$ represents the unit axis of rotation and $\phi(t) \in \mathbb{R}^1$ denotes the angle of rotation about $\mu(t)$ $(-\pi < \phi(t) < \pi)$ and are computed as follows

$$\phi = \cos^{-1}\left(\tfrac{1}{2}(\operatorname{tr}(\bar{R}) - 1)\right) \quad S(\mu) = \frac{\bar{R} - \bar{R}^T}{2\sin(\phi)} \tag{15}$$

where $S(\cdot) \in \mathbb{R}^{3\times3}$ denotes the skew-symmetric matrix form of a three element vector [16]. Given that the mobile robot moves on the XY plane, $\mu(t)$ and $\phi(t)$ take the following simplified form

$$\mu = \begin{bmatrix} 0 & 0 & 1 \end{bmatrix}^T \quad \phi = \theta_{CL} - \theta_{CL^*} \tag{16}$$

where $\theta_{ij}(t) \in \mathbb{R}^1$ is the right handed rotation about the z-axis that aligns the orientation of frame i with frame j (we assume $-\pi < \theta_{ij}(t) < \pi$). Hence, for our system only the third component of $e_\theta(t)$, denoted by $e_{\theta Z}(t) \in \mathbb{R}^1$, is non-zero and has the following form

$$\begin{aligned} e_\theta &= \begin{bmatrix} 0 & 0 & e_{\theta Z} \end{bmatrix}^T \\ e_{\theta Z} &= \theta_{CL} - \theta_{CL^*}. \end{aligned} \tag{17}$$

This form of $e_\theta(t)$ is useful for control design. By taking the time derivative of (14), the open loop dynamics of the orientation error can be expressed as follows

$$\begin{aligned} \dot{e}_\theta &= L_\omega \omega_{CL}^C \\ &= -L_\omega R_F^C(\omega_{IC}^F) + L_\omega R_L^C \omega_{IL}^L \end{aligned} \tag{18}$$

where $L_\omega(t) \in \mathbb{R}^{3\times3}$ is a Jacobian-like matrix given as follows

$$\begin{aligned} L_\omega &= I_{3\times3} - \tfrac{\phi}{2}S(\mu) + \left(1 - \frac{sinc(\phi)}{sinc^2(\frac{\phi}{2})}\right) S(\mu)^2 \\ sinc(\phi) &\triangleq \frac{\sin(\phi)}{\phi}. \end{aligned} \tag{19}$$

The derivation of $L_\omega(t)$ is presented in detail in [10]. Using (1), (2) and (16), the expression in (18) can be simplified as follows

$$\dot{e}_\theta = \begin{bmatrix} 0 & 0 & -\omega_F - \omega_C + \omega_L \end{bmatrix}^T. \tag{20}$$

The position error is defined in terms of the measurable signal $\frac{1}{d^*}\bar{x}(t)$ from the vision system. We first define an auxiliary variable $x_h(t) \in \mathbb{R}^3$ as follows

$$x_h \triangleq \frac{1}{d^*}\bar{x}. \tag{21}$$

By taking the time derivative of (8), the open loop dynamics of $x_h(t)$ can be obtained as follows

$$\dot{x}_h = \frac{1}{d^*}\left(\dot{x}_{CL}^C - \dot{\bar{R}}\, x_{CL^*}^C\right). \tag{22}$$

For further development, we utilize the following properties of general rigid body motion [16]

$$\begin{aligned}
\dot{x}_{eb}^e &= R_b^e v_{eb}^b \\
\dot{R}_b^e &= S(\omega_{eb}^e)R_b^e = R_b^e S(\omega_{eb}^b)
\end{aligned} \tag{23}$$

where e and b can be any two frames of reference. Referring to Figure 1, $x_{CL}^C(t)$ can be expressed as

$$x_{CL}^C = R_F^C R_I^F\left(x_{IL}^I - x_{IF}^I\right) \tag{24}$$

and its time derivative, by using (23) and some manipulation, can be expressed as

$$\dot{x}_{CL}^C = R_I^C\left(v_{IL}^I - R_F^I v_{IF}^F\right) - S(\omega_{IC}^C)x_{CL}^C. \tag{25}$$

After substituting (25) into (22) and also using (23), we obtain the following expression

$$\begin{aligned}
d^*\dot{x}_h &= -R_F^C v_{IF}^F - d^* R_F^C S\left(\omega_{IC}^C\right) R_C^F x_h + \xi_1 \\
\xi_1 &\triangleq R_I^C v_{IL}^I - S(\omega_{IL}^C)\bar{R}x_{CL^*}^C
\end{aligned} \tag{26}$$

where $\xi_1 \in \mathbb{R}^3$ contains the unmeasurable quantities. Considering the form of (26) and utilizing Assumption 1, we can define the position error for our system, denoted by $\bar{x}_h(t) \in \mathbb{R}^3$, as follows

$$\bar{x}_h \triangleq R_C^F x_h. \tag{27}$$

The open-loop dynamics of the position error can be determined by taking the time derivative of (27) as follows

$$\dot{\bar{x}}_h = R_C^F \dot{x}_h + \dot{R}_C^F x_h. \tag{28}$$

After substituting (26) into (28), and utilizing (23), the following expression can be obtained

$$\begin{aligned}
\dot{\bar{x}}_h &= -\frac{1}{d^*}v_{IF}^F - S(\omega_{IF}^F)\bar{x}_h + \frac{1}{d^*}R_C^F \xi_1 \tag{29}\\
\bar{\xi}_1 &\triangleq \frac{1}{d^*}R_C^F \xi_1 \tag{30}
\end{aligned}$$

Given that the mobile robot and the leader move on the XY plane, $\bar{x}_h(t)$ and $\bar{\xi}_1(t)$ have the following form

$$\begin{aligned}
\bar{x}_h &= \begin{bmatrix} \bar{x}_{h1} & \bar{x}_{h2} & 0 \end{bmatrix}^T \\
\bar{\xi}_1 &= \begin{bmatrix} \bar{\xi}_{11} & \bar{\xi}_{12} & 0 \end{bmatrix}^T
\end{aligned} \tag{31}$$

where $\bar{x}_{h1}(t)$, $\bar{x}_{h2}(t)$, $\bar{\xi}_{11}(t)$, $\bar{\xi}_{12}(t) \in \mathbb{R}^1$. After using (1), the open loop dynamics of $\bar{x}_{h1}(t)$ and $\bar{x}_{h2}(t)$ can be expressed as follows

$$\begin{aligned}
\dot{\bar{x}}_{h1} &= -\frac{1}{d^*}v_F + \omega_F \bar{x}_{h2} + \bar{\xi}_{11} \\
\dot{\bar{x}}_{h2} &= -\omega_F \bar{x}_{h1} + \bar{\xi}_{12}.
\end{aligned} \tag{32}$$

B. Closed-Loop Error System

First we define auxiliary error signals, denoted by $e_1(t)$, $e_2(t) \in \mathbb{R}^1$, as follows

$$\begin{aligned}
e_1 &= \bar{x}_{h1} + \delta_0 \\
e_2 &= \bar{x}_{h2}
\end{aligned} \tag{33}$$

where $\delta_0 \in \mathbb{R}^1$ is a positive design constant. Based on the open-loop dynamics (20) and (32), and the subsequent stability analysis, the control inputs $v_F(t)$, $\omega_F(t)$ and $\omega_C(t)$ are designed as follows

$$\begin{aligned}
v_F &= k_v e_1 \\
\omega_F &= -k_\omega e_2 \\
\omega_C &= \omega_F + k_\theta e_{\theta Z}
\end{aligned} \tag{34}$$

where k_v, k_ω, $k_\theta \in \mathbb{R}^1$ are positive tunable gains. Given these control inputs, the closed-loop dynamics of $e_1(t)$, $e_2(t)$ and $e_{\theta Z}(t)$ can be expressed as follows

$$\begin{aligned}
\dot{e}_{\theta Z} &= -k_\theta e_{\theta Z} + \omega_L \\
d^*\dot{e}_1 &= -k_v e_1 - k_\omega d^* e_2^2 + d^*\bar{\xi}_{11} \\
d^*\dot{e}_2 &= d^* k_\omega e_1 e_2 - k_\omega d^* \delta_0 e_2 + d^*\bar{\xi}_{12}.
\end{aligned} \tag{35}$$

IV. STABILITY ANALYSIS

Theorem 1: The follower's translational and rotational velocities, and the pan velocity of the camera, designed in (34), guarantee uniform ultimate boundedness (UUB) of the position error signal $\bar{x}_h(t)$ and the orientation error signal $e_\theta(t)$ in the neighborhood of zero in the following sense

$$\|\bar{x}_h(t)\|,\, \|e_\theta(t)\| \leq \alpha_1 \exp(-\alpha_2 t) + \alpha_3 \tag{36}$$

where α_1, α_2, $\alpha_3 \in \mathbb{R}^1$ are variable, positive constants.

Proof: We choose the following non-negative scalar function as the Lyapunov candidate

$$V = \frac{1}{2}e_{\theta Z}^2 + \frac{d^*}{2}e_1^2 + \frac{d^*}{2}e_2^2. \tag{37}$$

After taking the time derivative of (37) and substituting the closed-loop dynamics for $\dot{e}_\theta(t)$, $\dot{e}_1(t)$ and $\dot{e}_2(t)$ from (35), the following inequality can be obtained

$$\begin{aligned}
\dot{V} \leq\ & -k e_{\theta Z}^2 - k e_1^2 - k d^* \delta_0 e_2^2 - k_{\theta 1} e_{\theta Z}^2 + |e_{\theta Z}|\,|\beta_1| \\
& -k_{v1} e_1^2 + d^*\,|e_1|\,|\beta_2| - k_{\omega 1} d^* \delta_0 e_2^2 + d^*\,|e_2|\,|\beta_3|
\end{aligned} \tag{38}$$

where k, $k_{\theta 1}$, k_{v1}, $k_{\omega 1} \in \mathbb{R}^1$ are positive constants such that $k_\theta = k + k_{\theta 1}$, $k_v = k + k_{v1}$, $k_\omega = k + k_{\omega 1}$, and we have utilized Assumption 2 to upper bound $\omega_L(t)$, $\bar{\xi}_{11}(t)$, $\bar{\xi}_{12}(t)$ by positive constants, denoted by β_1, β_2, $\beta_3 \in \mathbb{R}^1$, as follows

$$\begin{aligned}
|\omega_L| &\leq \beta_1 \\
|\bar{\xi}_{11}| &\leq \beta_2 \\
|\bar{\xi}_{12}| &\leq \beta_3.
\end{aligned} \tag{39}$$

By using Young's Inequality [7], the last six terms of (38) can be upper bounded as follows

$$\begin{aligned}
|e_{\theta Z}|\,(|\beta_1| - k_{\theta 1}|e_{\theta Z}|) &< \frac{|\beta_1|^2}{k_{\theta 1}} \\
d^*\,|e_1|\left(|\beta_2| - \frac{k_{v1}}{d^*}|e_1|\right) &< \frac{d^{*2}|\beta_2|^2}{k_{v1}} \\
d^*\,|e_2|\,(|\beta_3| - k_{\omega 1}\delta_0|e_2|) &< \frac{d^*|\beta_3|^2}{k_{\omega 1}\delta_0}.
\end{aligned} \tag{40}$$

From (38) and (40), $\dot{V}(t)$ can be further upper bounded as follows

$$\dot{V} \leq -ke_{\theta Z}^2 - ke_1^2 - kd^*\delta_0 e_2^2 + \varepsilon \tag{41}$$

where $\varepsilon \triangleq \frac{|\beta_1|^2}{k_{\theta 1}} + \frac{d^{*2}|\beta_2|^2}{k_{v1}} + \frac{d^*|\beta_3|^2}{k_{\omega 1}\delta_0} \in \mathbb{R}^1$. We can upper-bound $\bar{x}_h(t)$ and $e_\theta(t)$, by solving the above differential equation, as follows

$$\|\bar{x}_h(t)\|, \|e_\theta(t)\| \leq V(t) \leq \alpha_1 \exp(-\alpha_2 t) + \alpha_3 \tag{42}$$

where $\alpha_1, \alpha_2, \alpha_3 \in \mathbb{R}^1$ are positive constants defined such that

$$
\begin{aligned}
\alpha_1 &= V(0) \\
\alpha_2 &= \frac{\min(k, kd^*\delta_0)}{\max\left(\frac{1}{2}, \frac{d^*}{2}\right)} \\
\alpha_3 &= \frac{\varepsilon}{\alpha_2}.
\end{aligned} \tag{43}
$$

The form of (36) follows directly from (42).

We now verify the boundedness of all signals in the system. From (37) and (41), $e_\theta(t), e_1(t), e_2(t) \in \mathcal{L}_\infty$. Hence, from (33), $\bar{x}_h(t) \in \mathcal{L}_\infty$, and from, (27) $x_h(t) \in \mathcal{L}_\infty$. It can be seen from (8) and (21) that $x_{CL}^C(t) \in \mathcal{L}_\infty$. From Assumption 2 and (24), $x_{IF}^I(t) \in \mathcal{L}_\infty$. Also, based on the control design in (34), $v_{IF}^F(t), \omega_{IF}^F(t), \omega_{FC}^F(t) \in \mathcal{L}_\infty$. Consequently, from (20), $\dot{e}_\theta(t) \in \mathcal{L}_\infty$. From (18), $\omega_{IC}^C(t) \in \mathcal{L}_\infty$. Therefore, $\dot{x}_h(t) \in \mathcal{L}_\infty$ (see (26)) and from (28) $\dot{\bar{x}}_h(t) \in \mathcal{L}_\infty$. Hence, all signals in the system remain bounded during closed-loop operation.

V. Simulation Results

We developed a simulation for validation of the leader/follower algorithm in C++ utilizing QMotor [2], a real-time control development environment for the QNX Operating System. Four coplanar feature points at the corners of a square fixed vertically on the leader formed the set of tracked features. For the simulation, the image coordinates of these feature points as seen by the camera on the follower were obtained based on the kinematics of the vehicles and the camera. The homography matrix was decomposed into its constituent motion parameters using an implementation of the algorithm given in [5]. The leader moved in a circular trajectory on the XY plane and its motion was not nonholonomic because its feature plane was always parallel to the y-axis while in motion. The initial positions of the follower and the leader were set as $x_{IF}^I = \begin{bmatrix} 8.5 & -0.5 & 0 \end{bmatrix}^T$ and $x_{IL}^I = \begin{bmatrix} 10 & 0 & 0 \end{bmatrix}^T$, respectively. The desired position of the follower was at 1 meter from the leader (i.e., $x_{CL^*}^C = \begin{bmatrix} 1 & 0 & 0 \end{bmatrix}^T$). The initial and desired orientation angles of the follower with respect to the leader were 20 degrees and 0 degrees, respectively. The trajectories of the leader and the follower are shown in Figure 2. The evolution of position and orientation errors with time is shown in Figure 3. The velocity control inputs remain within bounds as shown in Figure 4. For getting practical results, the magnitudes of the follower linear velocity, angular velocity and the PCU's angular velocity were saturated at 0.85 m/s, 0.3 rad/s and
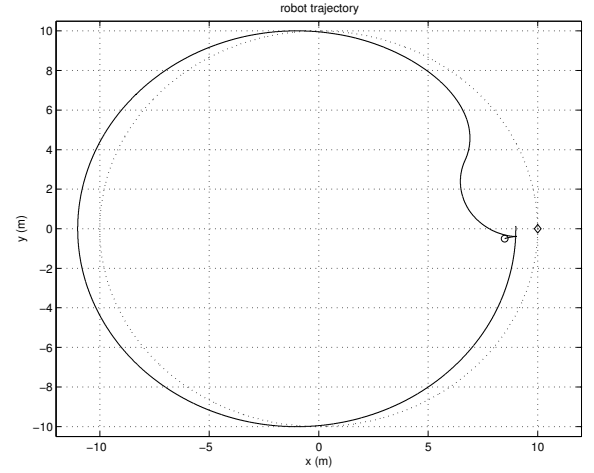

Fig. 2. Trajectories of the Leader ($\diamond$, dashed) and the Follower ($\circ$, solid).
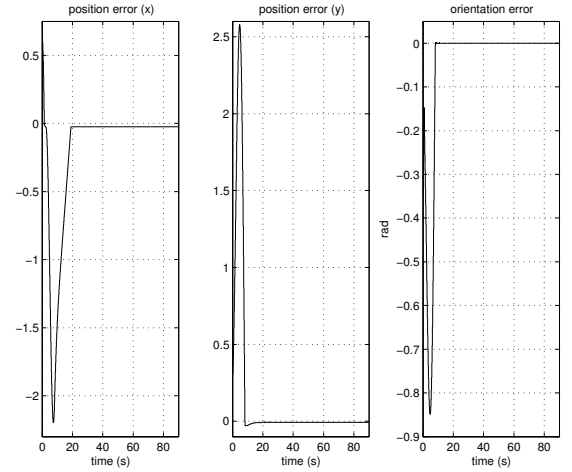

Fig. 3. The Position Errors (dimensionless) and the Orientation Error (radians).

0.75 rad/s, respectively. It is undesirable to start the motors in the follower robot with a high acceleration. Hence, a soft start was simulated by multiplying each of the velocity signals with a function of the form $(1 - \exp(-\alpha_s t))$. The following control parameters were selected upon trial and error

$$
\begin{aligned}
k_\theta &= 30, \quad k_v = 10, \quad k_\omega = 30, \\
\delta_0 &= 1 \times 10^{-3}.
\end{aligned} \tag{44}
$$

The follower took 20 seconds to attain the desired motion because of the initial error in position and orientation. It was observed that the follower traced a circle while maintaining the desired offset from the leader, which was the expected result.

VI. Conclusions

This paper presented a vision-based controller for a nonholonomic mobile robot with an onboard pan camera to follow a leader vehicle autonomously. Homography based
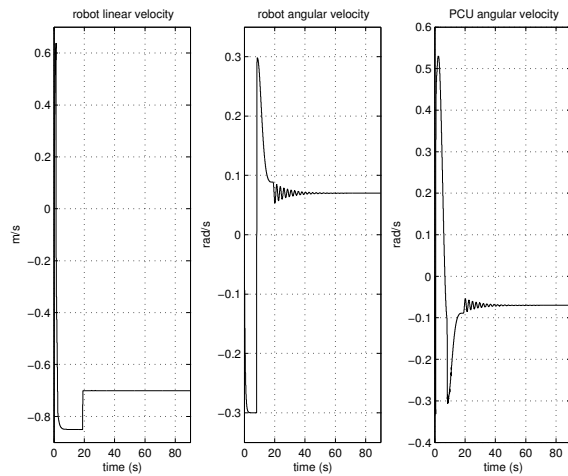
Fig. 4. The Follower Velocities and the PCU Velocity.

techniques were used to obtain relative position and orientation information from the monocular camera images, and the controller design was based on the Lyapunov method. The proposed controller was shown to achieve uniform ultimately bounded (UUB) tracking. Currently, we are working on the experimental verification of the proposed algorithm.

REFERENCES

[1] J. Chen, W. E. Dixon, D. M. Dawson, and M. McIntire, "Homography-based Visual Servo Tracking Control of a Wheeled Mobile Robot," IEEE Trans. on Robotics, Vol. 22, No. 2, pp. 406-415, 2006.

[2] N. Costescu, M. Loffler, M. Feemster, and D. M. Dawson, "QMotor 3.0 - An Objected Oriented System for PC Control Program Implementation and Tuning," Proc. of the American Control Conference, pp. 4526-4531, June 2001.

[3] A. Das, R. Fierro, V. Kumar, J. Ostrowski, J. Spletzer, and C. Taylor, "A Framework for Vision based Formation Control," IEEE Trans. on Robotics and Automation, Vol. 18, No. 5, pp. 813–825, 2002.

[4] J. Desai, J. Ostrowski, and V. Kumar, "Modeling and Control of Formations of Nonholonomic Mobile Robots," IEEE Trans. on Robotics and Automation, Vol. 17, No. 6, pp. 905–908, 2001.

[5] O. Faugeras, Three-Dimensional Computer Vision, The MIT Press, ISBN: 0262061589, 1993.

[6] T. I. Fossen, Marine Control Systems: Guidance, Navigation and Control of Ships, Rigs and Underwater Vehicles , Marine Cybernetics AS (Norway), ISBN: 8292356010, 2002.

[7] M. Krstić, I. Kanellakopoulos, and P. Kokotović, Nonlinear and Adaptive Control Design, New York, NY: John Wiley and Sons, 1995.

[8] Y. Ma, S. Soatto, J. Košecká, and S. Sastry, An Invitation to 3D Vision, Springer-Verlag, ISBN: 0387008934, 2003.

[9] J. Malik, C. J. Taylor, P. Mclauchlan, and J. Kosecká, "Development of Binocular Stereopsis for Vehicle Lateral Control," PATH MOU-257 Final Report, 1998.

[10] E. Malis, "Contributions à la modèlisation et à la commande en asservissement visuel," Ph.D. Thesis, University of Rennes I, IRISA, France, 1998.

[11] E. Malis and F. Chaumette, "2 1/2 D Visual Servoing with Respect to Unknown Objects Through a New Estimation Scheme of Camera Displacement," International Journal of Computer Vision, Vol. 37, No. 1, pp. 79–97, 2000.

[12] G. L. Mariottini, G. Pappas, D. Prattichizzo and K. Daniilidis, "Vision-based Localization of Leader-Follower Formations," IEEE Conf. on Decision and Control, pp. 635–640, Dec. 2005.

[13] O. A. A. Orqueda and R. Fierro, "Robust Vision-based Nonlinear Formation Control," Proc. of the American Control Conference, pp. 1422–1427, June 2006.

[14] D. A. Schoenwald, "AUVs: In Space, Air, Water, and on the Ground ," IEEE Control Systems Magazine, Vol. 20, No. 6, pp. 15–18, Dec. 2000.

[15] H. Sermeno-Villalta and J. Spletzer, "Vision-based Control of a Smart Wheelchair for the Automated Transport and Retrieval System," IEEE Int. Conf. on Robotics and Automation, pp. 3423-3428, May 2006.

[16] M. W. Spong, and M. Vidyasagar, Robot Dynamics and Control, John Wiley and Sons, ISBN: 047161243, 1989.

[17] D. P. Tsakiris, P. Rives and C. Samson, "Extending Visual Servoing Techniques to Nonholonomic Mobile Robots," The Confluence of Vision and Control, Eds. G. Hager, D. Kriegman and S. Morse, Lecture Notes in Control and Information Systems (LNCIS), Springer-Verlag, 1998

[18] R. Vidal, O. Shakernia, and S. Sastry, "Formation Control of Non-holonomic Mobile Robots with Omnidirectional Visual Servoing and Motion Segmentation," IEEE Int. Conf. on Robotics and Automation, pp. 584–589, Sept. 2003.